Nonlinear Dyn (2022) 108:4181–4194
https://doi.org/10.1007/s11071-021-06531-y

ORIGINAL PAPER

Bäcklund transformation, exact solutions and diverse interaction phenomena to a (3+1)-dimensional nonlinear evolution equation

Yu-Hang Yin · Xing Lü · Wen-Xiu Ma

Received: 11 March 2021 / Accepted: 8 May 2021 / Published online: 4 June 2021

Abstract Under investigation in this paper is a (3+1)-dimensional nonlinear evolution equation, which was proposed and analyzed to study features and properties of nonlinear dynamics in higher dimensions. Using the Hirota bilinear method, we construct a bilinear Bäcklund transformation, which consists of four equations and involves six free parameters. With test function method and symbolic computation, three sets of lump–kink solutions and new types of interaction solutions are derived, and figures are presented to reveal the interaction behaviors. Setting constraints to the new interaction solution via the test function expressed by "polynomial-cos-cosh," we simulate the periodic interaction phenomenon. Pfaffian solutions to the (3+1)-dimensional nonlinear evolution equation are obtained based on a set of linear partial differential conditions. According to our results, the diversity of solutions to the (3+1)-dimensional nonlinear evolution equation is revealed.

Keywords Bäcklund transformation · Symbolic computation · Lump–kink solutions · Interaction behaviors · Pfaffian solutions

Y.-H. Yin · X. Lü (✉)
Department of Mathematics, Beijing Jiaotong University, Beijing 100044, China
e-mail: XLV@bjtu.edu.cn

W.-X. Ma (✉)
Department of Mathematics, Zhejiang Normal University, Jinhua 321004, Zhejiang, China
e-mail: mawx@cas.usf.edu

W.-X. Ma
Department of Mathematics, King Abdulaziz University, Jeddah 21589, Saudi Arabia

W.-X. Ma
Department of Mathematics and Statistics, University of South Florida, Tampa, FL 33620, USA

W.-X. Ma
International Institute for Symmetry Analysis and Mathematical Modelling, Department of Mathematical Sciences, North-West University, Mafikeng Campus, Private Bag X 2046, Mmabatho 2735, South Africa

1 Introduction

Nonlinear evolution equations (NLEEs) play a significant role in the fields of engineering and mathematical physics involving fluid mechanics, plasma physics, optical fibers and nonlinear traffic flow theory [1–12]. As there are a variety of properties related to NLEEs, exact solutions have become more crucial and have attracted much attention [13–23]. In the past few decades, abundant effective methods have been proposed to solve NLEEs, such as the Hirota bilinear method [12], the inverse scattering method [12,24], the Darboux transform [12,25] and the Bäcklund transform [9,26]. Soliton solutions is a kind of special solution which are exponentially localized in certain directions [12]. Multi-soliton solutions generated from a combination of exponential waves to certain integrable nonlinear equations have been deduced, including the Korteweg–de Vries (KdV) equation, the Boussinesq equation and the Kadomtsev–Petviashvili (KP) equation [19,22,23,26–28]. Unlike soliton solutions, lump solutions are rationally localized in all directions of the space [19]. Using the Hirota bilinear method, Ablowitz and Satsuma firstly derived lump solutions to the KP equation in 1978 [20]. In 2015, Ma derived lump solutions to the (2+1)-dimensional KP equation through symbolic computation [19]. In recent years, interaction solutions including lump–kink solutions and lump–soliton solutions have become a hot topic [13–18,20,22]. Based on interaction solutions to NLEEs, a variety of complex interaction behaviors have been revealed, among which rogue wave is an important phenomenon [29–32]. According to research results in fields of oceanography, physics and engineering sciences, rogue wave gets its name from large spontaneous and unexpected water wave excitations which are great threat even to big ships [29,30]. It is implied by some researchers that rogue waves are the results of the interaction between a lump wave and a two-soliton wave [31,32]. With the application of symbolic computation and data processing techniques, the test function method has become a powerful way to investigate interaction solutions to NLEEs [13,14,16,17]. Using symbolic computation, we can construct test functions and obtain diverse exact solutions to NLEEs [13,14,16,17].

Multi-soliton solutions of many integrable bilinear equations can generally be expressed as determinants, such as Wronskian determinant and Grammian determinant [33–35]. Nevertheless, not all soliton equations have solutions of determinant-type and some equations have Pfaffian solutions [36,37]. For example, Wronskian solutions and Grammian solutions to the KP equation, Jimbo–Miwa (JM) equation and Sawada–Kotera (SK) equation have been deduced, while Pfaffian solutions to the B-type Kadomtsev–Petviashvili (B-KP) equation were firstly presented by Hirota [36,38–41]. We set A as an antisymmetric determinant of order $2n$,

$$A = \det(a_{jk}), 1 \leq j, k \leq 2n, \tag{1}$$

where $a_{jk} = -a_{kj}$. A can be expressed as the square of a Pfaffian which is of order n and can be denoted as $(1, 2, \ldots, 2n)$. Using Maya charts designed by Mikio Sato [12], we can illustrate Pfaffian identities vividly. Moreover, Pfaffian identities have a richer structure than determinants and are of great help to understand the algebraic properties and the structure of multi-soliton solutions [36].

In this paper, we will study a (3+1)-dimensional NLEE as

$$u_{yt} - u_{xxxy} - 3\,(u_x\,u_y)_x - 3\,u_{xx} + 3\,u_{zz} = 0, \tag{2}$$

which was firstly proposed in Ref. [42] The resonant behavior of multiple wave solutions has been discussed [19,42], and interaction solutions to the dimensionally reduced equation have been studied [43]. The KP equation has been fully analyzed and is widely applied in fluid mechanics, including researches on shallow water waves and rogue waves [44–46]. According to the composition structure of Eq. (2), which is similar to that of the KP equation, we can regard Eq. (2) as a generalized (3+1)-dimensional KP equation to study the complex and diverse characteristics. In order to study more properties of this (3+1)-dimensional NLEE, it is of vital importance to construct Bäcklund transformation (BT) and exact solutions.

The structure of this paper is as follows: In Sect. 2, we will transform Eq. (2) into bilinear form and a BT will be constructed. Based on the constructed BT, the one-soliton solution to Eq. (2) will be deduced. In Sect. 3, a new-type test function expressed by "polynomial-cos-cosh" will be constructed to derive exact solutions to Eq. (2). With the aid of maple, we aim at obtaining abundant interaction solutions to Eq. (2), including lump–kink solutions, periodic-rational solutions and double kinky-periodic-rational solutions. Based on the expression of the exact solutions, figures will be plotted and analysis will be made to display interaction phenomena among lump waves, kinky waves and periodic waves. In Sect. 4, Pfaffian solutions will be deduced and figures of one-, two- and three-soliton solutions will also be presented. Section 5 will be the concluding remarks.

2 Bilinear representation and BT

2.1 Bilinear Bäcklund transformation

Using the dependent variable transformation

$$u = 2(\ln f)_x,\ f = f(x, y, z, t), \tag{3}$$

, we transform Eq. (2) into the bilinear form

$$(D_t D_y - D_x^3 D_y - 3D_x^2 + 3D_z^2) f \cdot f = 0, \quad (4)$$

where $D_t D_y$, $D_x^3 D_y$, D_x^2 and D_z^2 are all bilinear derivative operators [12] defined by

$$D_x^\alpha D_y^\beta D_z^\gamma D_t^\delta (f \cdot g) = \left(\frac{\partial}{\partial x} - \frac{\partial}{\partial x'}\right)^\alpha \left(\frac{\partial}{\partial y} - \frac{\partial}{\partial y'}\right)^\beta \times \left(\frac{\partial}{\partial z} - \frac{\partial}{\partial z'}\right)^\gamma \left(\frac{\partial}{\partial t} - \frac{\partial}{\partial t'}\right)^\delta \times f(x, y, z, t) g(x', y', z', t')\Big|_{x'=x, y'=y, z'=z, t'=t}. \quad (5)$$

Based on the bilinear form Eq. (4), we consider

$$\begin{aligned} P \equiv & f^2 (D_t D_y - D_x^3 D_y - 3D_x^2 + 3D_z^2) g \cdot g \\ & - g^2 (D_t D_y - D_x^3 D_y - 3D_x^2 + 3D_z^2) f \cdot f, \end{aligned} \quad (6)$$

where $g = g(x, y, z, t)$ is another solution to Eq. (4).

Using the bilinear operator identities

$$\begin{aligned} & (D_y D_t g \cdot g) f^2 - (D_y D_t f \cdot f) g^2 = 2D_y (D_t g \cdot f) \cdot (gf), \\ & (D_x^2 g \cdot g) f^2 - (D_x^2 f \cdot f) g^2 = 2D_x (D_x g \cdot f) \cdot (gf), \\ & (D_z^2 g \cdot g) f^2 - (D_z^2 f \cdot f) g^2 = 2D_z (D_z g \cdot f) \cdot (gf), \\ & (D_x^3 D_y g \cdot g) f^2 - (D_x^3 D_y f \cdot f) g^2 = 2D_y (D_x^3 g \cdot f) \cdot (gf) \\ & \qquad - 6D_x (D_x D_y g \cdot f) \cdot (D_x g \cdot f), \\ & D_z (D_x^2 g \cdot f) \cdot (gf) = D_x [(D_x D_z g \cdot f) \cdot (gf) \\ & \qquad + (D_x g \cdot f) \cdot (D_y g \cdot f)], \end{aligned} \quad (7)$$

we can rewrite Eq. (6) as

$$\begin{aligned} P = & 2D_y (D_t g \cdot f - D_x^3 g \cdot f + \lambda_1 g f) \cdot (gf) \\ & + 6D_x (D_x D_y g \cdot f + \lambda_2 D_x g \cdot f + \lambda_3 g f) \cdot (D_x g \cdot f) \\ & + 6\lambda_3 D_x (D_x g \cdot f) \cdot (gf) - 6D_x (D_x g \cdot f + \lambda_4 g f) \cdot (gf) \\ & + 6D_z (D_z g \cdot f - \lambda_5 D_x^2 g \cdot f + \lambda_6 g f) \cdot (gf) \\ & + 6\lambda_5 D_x (D_x D_z g \cdot f) \cdot (gf) \\ & + 6\lambda_5 D_x (D_x g \cdot f) \cdot (D_z g \cdot f) \\ = & 2D_y ((D_t - D_x^3 + \lambda_1) g \cdot f) \cdot (gf) \\ & + 6D_z ((D_z - \lambda_5 D_x^2 + \lambda_6) g \cdot f) \cdot (gf) \\ & + 6D_x ((D_x D_y + \lambda_2 D_x - \lambda_5 D_z + \lambda_3) g \cdot f) \cdot (D_x g \cdot f) \\ & + 6D_x ((\lambda_5 D_x D_z + \lambda_3 D_x - D_x - \lambda_4) g \cdot f) \cdot (gf), \end{aligned} \quad (8)$$

where we have introduced six arbitrary coefficients λ_i $(i = 1, 2, 3, 4, 5, 6)$. Then, a BT associated with Eq. (4) can be constructed as

$$\begin{cases} B_1 g \cdot f = (D_t - D_x^3 + \lambda_1) g \cdot f = 0, \\ B_2 g \cdot f = (D_z - \lambda_5 D_x^2 + \lambda_6) g \cdot f = 0, \\ B_3 g \cdot f = (D_x D_y + \lambda_2 D_x + \lambda_3 - \lambda_5 D_z) g \cdot f = 0, \\ B_4 g \cdot f = (\lambda_5 D_x D_z + (\lambda_3 - 1) D_x - \lambda_4) g \cdot f = 0. \end{cases} \quad (9)$$

2.2 Soliton solution to Eq. (2)

Obviously, $f = 1$ is a solution to Eq. (4). Substituting $f = 1$ into Eq. (9), we obtain four linear partial differential equations as

$$\begin{cases} g_t - g_{xxx} + \lambda_1 g = 0, \\ g_z - \lambda_5 g_{xx} + \lambda_6 g = 0, \\ g_{xy} + \lambda_2 g_x - \lambda_5 g_z + \lambda_3 g = 0, \\ \lambda_5 g_{xz} + (\lambda_3 - 1) g_x - \lambda_4 g = 0. \end{cases} \quad (10)$$

We assume that exponential solutions to Eq. (10) are as follows

$$g = 1 + \varepsilon e^{m_1 x + m_2 y + m_3 z + m_4 t}, \quad (11)$$

where m_1, m_2, m_3 and m_4 are all constants.

Selecting $\lambda_1 = \lambda_3 = \lambda_4 = \lambda_6 = 0$ and solving Eq. (10), we have

$$m_4 = m_1^3, \lambda_2 = \frac{m_3^2}{m_1^3} - m_2, \lambda_5 = \frac{m_3}{m_1^2}. \quad (12)$$

Now, exponential solutions to Eq. (10) are derived as

$$g = 1 + \varepsilon e^{m_1 x + m_2 y + m_3 z + m_1^3 t} \quad (13)$$

and the soliton solution to Eq. (2) can be written as

$$u = 2(\ln g)_x = \frac{2m_1 \varepsilon e^{m_1 x + m_2 y + m_3 z + m_1^3 t}}{1 + \varepsilon e^{m_1 x + m_2 y + m_3 z + m_1^3 t}}. \quad (14)$$

Selecting appropriate parameters, we obtain the figure of the one-soliton solution to Eq. (2) as plotted in Fig. 1.

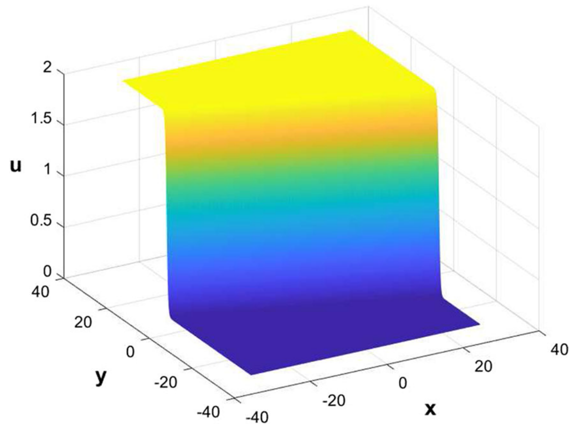

Fig. 1 The one-soliton solution to Eq. (2) via Eq. (14) with $m_1 = 1, m_2 = 3, m_3 = 2, z = 0, t = 0$ and $\varepsilon = 1$

3 Interaction solutions and interaction behaviors

3.1 Lump–kink solutions to Eq. (2)

In this section, we aim at obtaining lump–kink solutions to Eq. (2). According to the structure of lump–kink solutions, we assume the solution to Eq. (4) is in the form of

$$f = g^2 + h^2 + e^{\eta} + a_{16}, \tag{15}$$

where $g = a_1x + a_2y + a_3z + a_4t + a_5$, $h = a_6x + a_7y + a_8z + a_9 + a_{10}$, $\eta = a_{11}x + a_{12}y + a_{13}z + a_{14}t + a_{15}$, $a_{16} \geq 0$ and a_i $(1 \leq i \leq 16)$ are some constants to be determined.

With symbolic computation, we directly substitute Eq. (15) into Eq. (4) and derive the following three sets of a_i $(1 \leq i \leq 16)$.

Case 1

$$\begin{aligned}\{&a_1 = a_1, a_2 = 0, a_3 = -a_1, a_4 = \frac{6a_1a_8}{a_7}, a_5 = a_5,\\ &a_6 = 0, a_7 = a_7, a_8 = a_8, a_9 = -\frac{3a_8^2}{a_7}, a_{10} = a_{10},\\ &a_{11} = a_{11}, a_{12} = 0, a_{13} = -a_{11},\\ &a_{14} = -\frac{a_{11}(a_{11}^2a_7 - 6a_8)}{a_7}, a_{15} = a_{15}, a_{16} = a_{16}\},\end{aligned} \tag{16}$$

where $a_1, a_5, a_7, a_8, a_{10}, a_{11}, a_{15}, a_{16}$ are real constants and conditions are given as

$$\{a_1a_7a_{11} \neq 0\,, a_{16} \geq 0\} \tag{17}$$

to guarantee the well-definedness of f.

Substituting parameters of Eq. (16) into Eq. (15), we have

$$\begin{aligned}f =& (a_1x - a_1z + \frac{6a_1a_8}{a_7}t + a_5)^2\\ &+ (a_7y + a_8z - \frac{3a_8^2}{a_7}t + a_{10})^2\\ &+ e^{a_{11}x - a_{11}z - \frac{a_{11}(a_{11}^2a_7 - 6a_8)}{a_7}t + a_{15}} + a_{16},\end{aligned} \tag{18}$$

which leads to the lump–kink solution to Eq. (2) as

$$u = \frac{2(2a_1A_1 + a_{11}e^{C_1})}{A_1^2 + B_1^2 + e^{C_1} + a_{16}}, \tag{19}$$

where $A_1 = a_1x - a_1z + \frac{6a_1a_8}{a_7}t + a_5$, $B_1 = a_7y + a_8z - \frac{3a_8^2}{a_7}t + a_{10}$ and $C_1 = a_{11}x - a_{11}z - \frac{a_{11}(a_{11}^2a_7 - 6a_8)}{a_7}t + a_{15}$.

Case 2

$$\begin{aligned}\{&a_1 = a_1, a_2 = 0, a_3 = a_1, a_4 = -\frac{6a_1a_8}{a_7}, a_5 = a_5,\\ &a_6 = 0, a_7 = a_7, a_8 = a_8, a_9 = -\frac{3a_8^2}{a_7}, a_{10} = a_{10},\\ &a_{11} = a_{11}, a_{12} = 0, a_{13} = a_{11},\\ &a_{14} = -\frac{a_{11}(a_{11}^2a_7 + 6a_8)}{a_7}, a_{15} = a_{15}, a_{16} = a_{16}\},\end{aligned} \tag{20}$$

where $a_1, a_5, a_7, a_8, a_{10}, a_{11}, a_{15}, a_{16}$ are real constants and conditions are given as

$$\{a_1a_7a_{11} \neq 0\,, a_{16} \geq 0\} \tag{21}$$

to guarantee the well-definedness of f.

Substituting parameters of Eq. (20) into Eq. (15), we have

$$f=(a_1x+a_1z-\frac{6a_1a_8}{a_7}t+a_5)^2 + (a_7y+a_8z-\frac{3a_8^2}{a_7}t+a_{10})^2 + e^{a_{11}x+a_{11}z-\frac{a_{11}(a_{11}^2a_7+6a_8)}{a_7}t+a_{15}}+a_{16}, \tag{22}$$

which leads to the lump–kink solution to Eq. (2) as

$$u=\frac{2(2a_1A_2+a_{11}e^{C_2})}{A_2^2+B_2^2+e^{C_2}+a_{16}}, \tag{23}$$

where $A_2=a_1x+a_1z-\frac{6a_1a_8}{a_7}t+a_5$, $B_2=a_7y+a_8z-\frac{3a_8^2}{a_7}t+a_{10}$ and $C_2=a_{11}x+a_{11}z-\frac{a_{11}(a_{11}^2a_7+6a_8)}{a_7}t+a_{15}$.

Case 3

$$\{a_1=0, a_2=0, a_3=a_3, a_4=\frac{6a_3^3a_8}{a_{12}^2a_6^3}, a_5=a_5, a_6=a_6, a_7=-\frac{a_{12}^2a_6^3}{a_3^2}, a_8=a_8, a_9=-\frac{3a_3^2(a_3^2+a_6^2-a_8^2)}{a_{12}^2a_6^3}, a_{10}=a_{10}, a_{11}=-\frac{a_3^2}{a_{12}a_6^2}, a_{12}=a_{12}, a_{13}=-\frac{a_8a_3^2}{a_{12}a_6^3}, a_{14}=\frac{a_3^4(a_3^2+3a_6^2-3a_8^2)}{a_{12}^3a_6^6}, a_{15}=a_{15}, a_{16}=a_{16}\}, \tag{24}$$

where $a_3, a_5, a_6, a_8, a_{12}, a_{15}, a_{16}$ are real constants and conditions are given as

$$\{a_3a_6a_{12}\neq 0, a_{16}\geq 0\} \tag{25}$$

to guarantee the well-definedness of f.

Substituting parameters of Eq. (24) into Eq. (15), we have

$$f=(a_3z+\frac{6a_3^3a_8}{a_{12}^2a_6^3}t+a_5)^2+(a_6x-\frac{a_{12}^2a_6^3}{a_3^2}y + a_8z-\frac{3a_3^2(a_3^2+a_6^2-a_8^2)}{a_{12}^2a_6^3}t+a_{10})^2 + e^{-\frac{a_3^2}{a_{12}a_6^2}x+a_{12}y-\frac{a_8a_3^2}{a_{12}a_6^3}z+\frac{a_3^4(a_3^2+3a_6^2-3a_8^2)}{a_{12}^3a_6^6}t+a_{15}}+a_{16}, \tag{26}$$

which leads to the lump–kink solution to Eq. (2) as

$$u=\frac{2(2a_6B_3-\frac{a_3^2}{a_{12}a_6^2}e^{C_3})}{A_3^2+B_3^2+e^{C_3}+a_{16}}, \tag{27}$$

where $A_3=a_3z+\frac{6a_3^3a_8}{a_{12}^2a_6^3}t+a_5$, $B_3=a_6x-\frac{a_{12}^2a_6^3}{a_3^2}y+a_8z-\frac{3a_3^2(a_3^2+a_6^2-a_8^2)}{a_{12}^2a_6^3}t+a_{10}$ and $C_3=-\frac{a_3^2}{a_{12}a_6^2}x+a_{12}y-\frac{a_8a_3^2}{a_{12}a_6^3}z+\frac{a_3^4(a_3^2+3a_6^2-3a_8^2)}{a_{12}^3a_6^6}t+a_{15}$.

Based on the expression of u given by Eq. (19), we take a selection of the parameters $a_i(1\leq i\leq 16)$ and obtain figures of lump–kink solutions.

When $\frac{a_{11}(a_{11}^2a_7-6a_8)}{a_7}>0$, we obtain $\lim_{t\to+\infty}u=0$, $\lim_{t\to+\infty}\frac{e^{C_1}}{A_1^2+B_1^2}=0$, $\lim_{t\to-\infty}u=2a_{11}$ and $\lim_{t\to-\infty}\frac{A_1^2+B_1^2}{e^{C_1}}=0$. In this case, when $t\to-\infty$, the kinky wave plays the dominant role and the lump wave plays the dominant role when $t\to+\infty$.

When $\frac{a_{11}(a_{11}^2a_7-6a_8)}{a_7}<0$, we obtain $\lim_{t\to-\infty}u=0$, $\lim_{t\to-\infty}\frac{e^{C_1}}{A_1^2+B_1^2}=0$, $\lim_{t\to+\infty}u=2a_{11}$ and $\lim_{t\to+\infty}\frac{A_1^2+B_1^2}{e^{C_1}}=0$. In this case, when $t\to+\infty$, the kinky wave plays the dominant role and the lump wave plays the dominant role when $t\to-\infty$.

As we can see in Fig. 2, there are interaction behaviors between lump and kink. The wave consists of two parts, including the lump wave and the kinky wave. With the increase of t, the lump first appears on one side of the kinky wave, and then, it begins to move toward the other one and is gradually swallowed. Finally, only the kinky wave exists.

3.2 New interaction solutions to Eq. (2)

In this section, we construct a test function expressed by "polynomial-cos-cosh" to study diverse exact solution to Eq. (2) and abundant interaction behaviors. It is assumed that solutions to Eq. (4) are in the form of

$$f=p^2+q^2+k\cosh(\xi)+l\cos(\gamma)+b_{21}, \tag{28}$$

where $p=b_1x+b_2y+b_3z+b_4t+b_5$, $q=b_6x+b_7y+b_8z+b_9+b_{10}$, $\xi=b_{11}x+b_{12}y+b_{13}z+b_{14}t+b_{15}$, $\gamma=b_{16}x+b_{17}y+b_{18}z+b_{19}t+b_{20}$, $b_{21}\geq|l|$, $k>0$ and $b_i(1\leq i\leq 21)$, k, l are some constants to be determined.

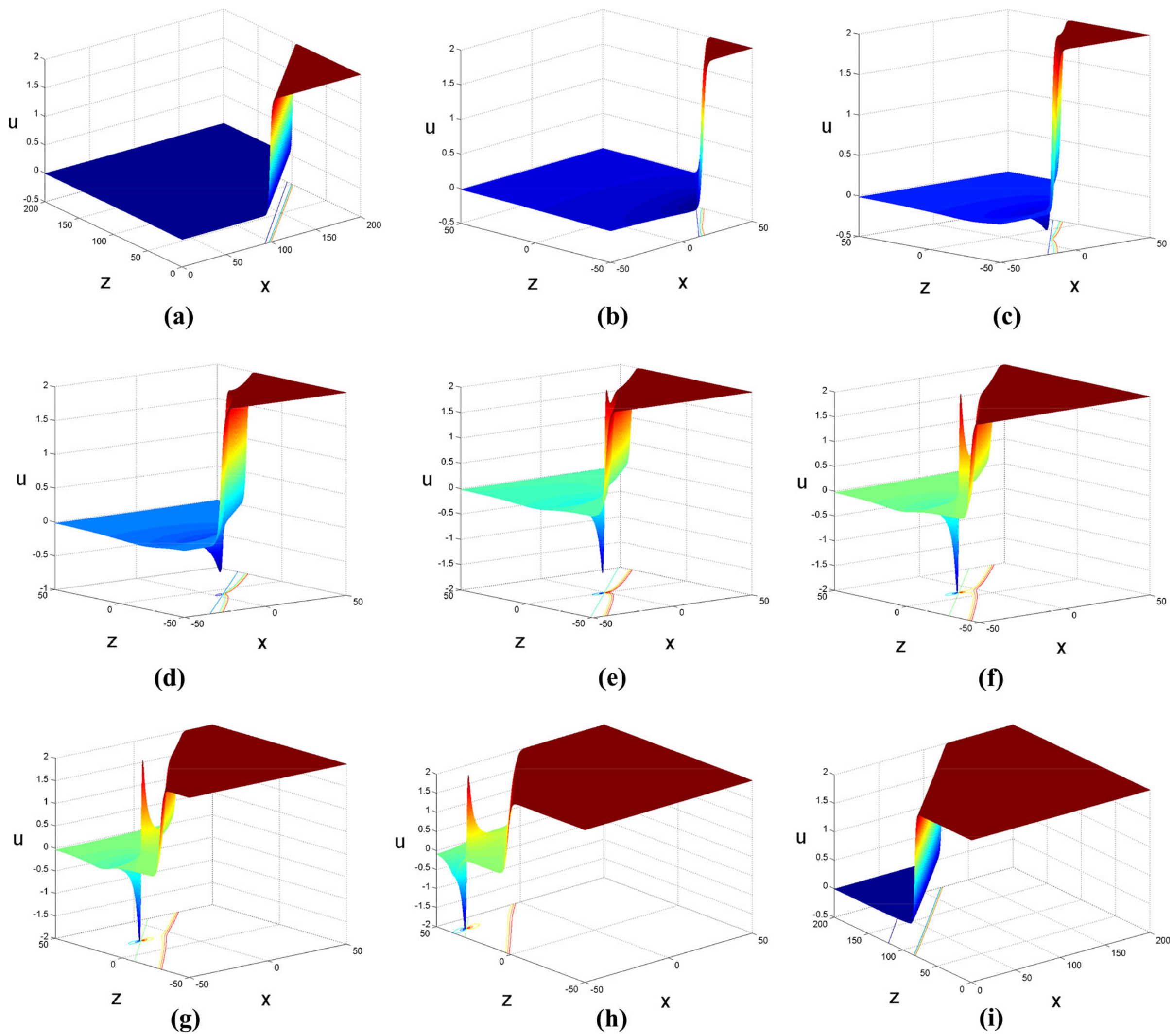

Fig. 2 The 3-dimensional plot of u via Eq. (19) at **a** $t = -30$, **b** $t = -20$, **c** $t = -10$, **d** $t = -5$, **e** $t = 0$, **f** $t = 5$, **g** $t = 10$, **h** $t = 20$ and **i** $t = 30$ with $y = 0$, $a_1 = 1$, $a_5 = 1$, $a_7 = 3$, $a_8 = 2$, $a_{10} = 1$, $a_{11} = 1$, $a_{15} = 1$ and $a_{16} = 1$

With symbolic computation, we directly substitute Eq. (28) into Eq. (4) and derive the following set of b_i $(1 \leq i \leq 21)$, k and l.

$$\begin{aligned}
&\{b_1 = b_1, b_2 = 0, b_3 = b_1, b_4 = -\frac{6b_1b_8}{b_7}, b_5 = b_5,\\
&b_6 = 0, b_7 = b_7, b_8 = b_8, b_9 = -\frac{3b_8^2}{b_7}, b_{10} = b_{10},\\
&b_{11} = b_{11}, b_{12} = 0, b_{13} = b_{11},\\
&b_{14} = -\frac{b_{11}(b_{11}^2 b_7 + 6b_8)}{b_7}, b_{15} = b_{15},\\
&b_{16} = b_{16}, b_{17} = 0, b_{18} = b_{16},\\
&b_{19} = \frac{b_{16}(b_{16}^2 b_7 - 6b_8)}{b_7}, b_{20} = b_{20},\\
&b_{21} = b_{21}, k = k, l = l\},
\end{aligned} \tag{29}$$

where $b_1, b_5, b_7, b_8, b_{10}, b_{11}, b_{16}, b_{20}, b_{21}, k, l$ are real constants and conditions are given as

$$\{b_7 l \neq 0, k > 0, b_{21} \geq |l|\}. \tag{30}$$

Substituting parameters of Eq. (29) into Eq. (28), we have

$$f = (b_1x + b_1z - \frac{6b_1b_8}{b_7}t + b_5)^2 + (b_7y + b_8z - \frac{3b_8^2}{b_7}t + b_{10})^2 + k\cosh(b_{11}x + b_{11}z - \frac{b_{11}(b_{11}^2b_7 + 6b_8)}{b_7}t + b_{15}) + l\cos(b_{16}x + b_{16}z + \frac{b_{16}(b_{16}^2b_7 - 6b_8)}{b_7}t + b_{20}) + b_{21}, \quad (31)$$

which leads to the exact solution to Eq. (2) as

$$u = \frac{2(2b_1A_4 + b_{11}k\cosh(C_4) + b_{16}\cos(D))}{A_4^2 + B_4^2 + k\cosh(C_4) + \cos(D) + b_{21}}, \quad (32)$$

where $A_4 = b_1x + b_1z - \frac{6b_1b_8}{b_7}t + b_5$, $B_4 = b_7y + b_8z - \frac{3b_8^2}{b_7}t + b_{10}$, $C_4 = b_{11}x + b_{11}z - \frac{b_{11}(b_{11}^2b_7+6b_8)}{b_7}t + b_{15}$ and $D = b_{16}x + b_{16}z + \frac{b_{16}(b_{16}^2b_7-6b_8)}{b_7}t + b_{20}$.

Based on the expression of u given by Eq. (32), we can obtain $\lim_{t\to\pm\infty} u = 2b_{11}$ and $\lim_{t\to\pm\infty} \frac{A_4^2+B_4^2+\cos(D)}{\cosh(C_4)} = 0$. Taking a selection of the parameters b_i $(1 \le i \le 21)$, k and l, figures of the constructed solutions are derived.

As we can see in Figs. 3 and 4, the interaction phenomenon involves three kinds of different waves, including the two-kinky wave, the lump wave and the trigonometric-type wave. With the increase of t, the lump wave first appears on one side of the two-kinky wave; then, it begins to move to the other side, and finally, the lump wave is swallowed. The waveform presented in Fig. 3 is different from that of the lump-2-kink solution and it reveals the existence of the trigonometric-type wave.

For further investigation on the new-type interaction solution, we set different values to parameters and rewrite Eq. (31) and Eq. (32) as

$$f = b_5^2 + (b_7y + b_8z - \frac{3b_8^2}{b_7}t + b_{10}^2)^2 + k\cosh(b_{11}x + b_{11}z - \frac{b_{11}(b_{11}^2b_7 + 6b_8)}{b_7} + b_{15}) + l\cos(b_{16}x + b_{16}z + \frac{b_{16}(b_{16}^2b_7 - 6b_8)}{b_7}t + b_{20}) + b_{21},$$

$$u = \frac{2(b_{11}k\cosh(C_4) + b_{16}\cos(D))}{A_4^2 + B_4^2 + k\cosh(C_4) + \cos(D) + b_{21}}, \quad (33)$$

where $b_1 = 0$, $A_4 = b_1x + b_1z - \frac{6b_1b_8}{b_7}t + b_5$, $B_4 = b_7y + b_8z - \frac{3b_8^2}{b_7}t + b_{10}$, $C_4 = b_{11}x + b_{11}z - \frac{b_{11}(b_{11}^2b_7+6b_8)}{b_7}t + b_{15}$ and $D = b_{16}x + b_{16}z + \frac{b_{16}(b_{16}^2b_7-6b_8)}{b_7}t + b_{20}$.

When $b_5 = 1, b_7 = 3, b_8 = 2, b_{10} = 1, b_{11} = 1, b_{15} = 1, b_{16} = 1, b_{20} = 1, b_{21} = 3, k = 0.01, l = 2$ and $z = 0$, the solution to Eq. (2) is deduced as

$$u = \frac{2(-0.01\sinh(-x + 5t - 1) + 2\sin(-x + 3t - 1))}{(3y - 4t + 1)^2 + 0.01\cosh(x - 5t + 1) + 2\cos(x - 3t + 1) + 4}. \quad (34)$$

Based on the expression of u given by Eq. (34), we select different values of t and figures of the exact solutions to Eq. (2) are presented in Fig. 5.

As we can see in Fig. 5, there are interaction behaviors between the x-periodic-rational wave and the kinky wave. The x-periodic-rational wave first appears on one side of the two-kinky wave; then, it begins to move to the other side, and finally, the x-periodic-rational wave is swallowed. The value of the period on the x-axis is

$$T = \frac{2\pi}{b_{16}} = 2\pi. \quad (35)$$

4 Pfaffian solutions

The Pfaffian entry (i, j) is defined by

$$(i, j) = c_{ij} + \int^x \phi_{i,x}\phi_j - \phi_i\phi_{j,x}\,dx, \quad (36)$$

where $c_{ij} (1 \le i, j \le 2N)$ are constants and satisfy the condition $c_{ij} = -c_{ji}$, and ϕ_i is a function of the scaled space coordinates x, y, z and time t. ϕ_i's satisfy the following linear partial differential condition

$$\frac{\partial}{\partial y}\phi_i = (k^2 - 1)\int^x \phi_i\,dx, \quad \frac{\partial}{\partial z}\phi_i = k\frac{\partial}{\partial x}\phi_i, \quad \frac{\partial}{\partial t}\phi_i = \frac{\partial^3}{\partial x^3}\phi_i, \quad (37)$$

where $k \ne 0$ and $k \ne \pm 1$.

Theorem 4.1 *If ϕ_i meets the linear partial differential condition Eq. (37), then the Pfaffian f_N is the solution to Eq. (4). Using the transformation $u = 2(\ln f_N)_x$, we can obtain the solution to Eq. (2).*

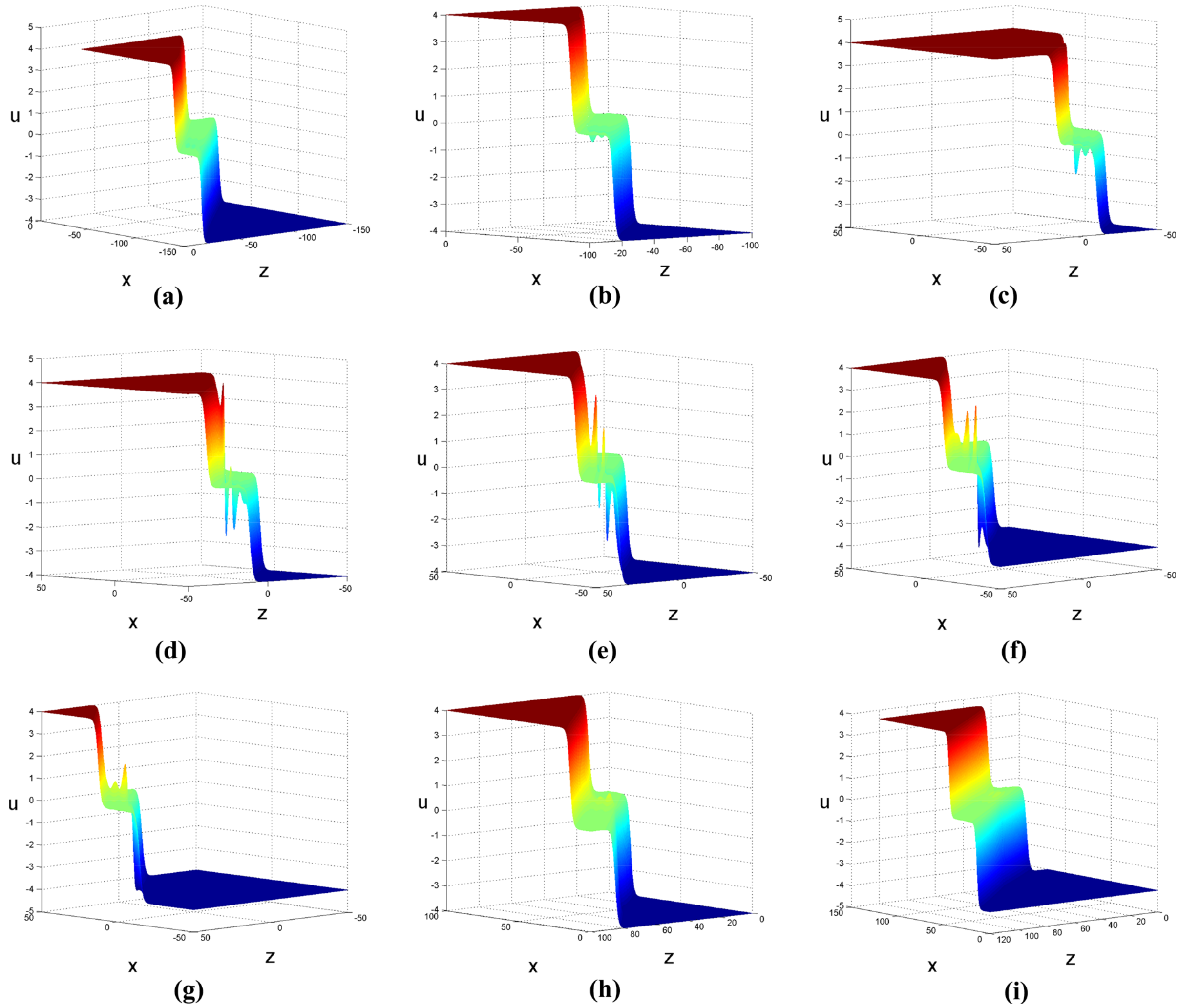

Fig. 3 The 3-dimensional plot of u via Eq. (32) at **a** $t=-30$, **b** $t=-20$, **c** $t=-10$, **d** $t=-5$, **e** $t=0$, **f** $t=5$, **g** $t=10$, **h** $t=20$ and **i** $t=30$ with $y=0$, $a_1=1$, $a_5=1$, $a_7=3$, $a_8=2$, $a_{10}=1$, $a_{11}=1$, $a_{15}=1$, $a_{16}=1$, $a_{20}=1$, $a_{21}=10$, $k=0.01$ and $l=8$

Proof Using the linear partial differential condition presented in Eq. (37), we obtain derivatives of the entries (i,j) as

$$
\begin{aligned}
\frac{\partial}{\partial x}(i,j) &= \phi_{i,x}\phi_j-\phi_i\phi_{j,x}=(d_0,d_1,i,j),\\
\frac{\partial}{\partial y}(i,j) &= \int^x(\phi_{i,xy}\phi_j+\phi_{i,x}\phi_{j,y}-\phi_{i,y}\\
&\quad\times\phi_{j,x}-\phi_i\phi_{j,xy})dx=\phi_i\phi_{j,y}-\phi_{i,y}\phi_j\\
&=(k^2-1)(d_{-1},d_0,i,j),\\
\frac{\partial}{\partial z}(i,j) &= k(\phi_{i,x}\phi_j-\phi_i\phi_{j,x})=k(d_0,d_1,i,j),
\end{aligned}
$$

$$
\begin{aligned}
\frac{\partial}{\partial t}(i,j) &= \int^x(\phi_{i,xt}\phi_j+\phi_{i,x}\phi_{j,t}-\phi_{i,t}\phi_{j,x}-\phi_i\phi_{j,xt})\\
&=k(\phi_{i,xxx}\phi_j-\phi_i\phi_{j,xxx}\\
&\quad-2(\phi_{i,xx}\phi_{j,x}-\phi_{i,x}\phi_{j,xx}))\\
&=k[(d_0,d_3,i,j)-2(d_1,d_2,i,j)],
\end{aligned}
\qquad (38)
$$

where

$$
(d_{-1},i)=\int^x\phi_i\,dx,\quad (d_n,i)=\frac{\partial^n}{\partial x^n}\phi_i,
$$
$$
(d_m,d_n)=0,\ (m,n=-1,0,1,2,3). \qquad (39)
$$

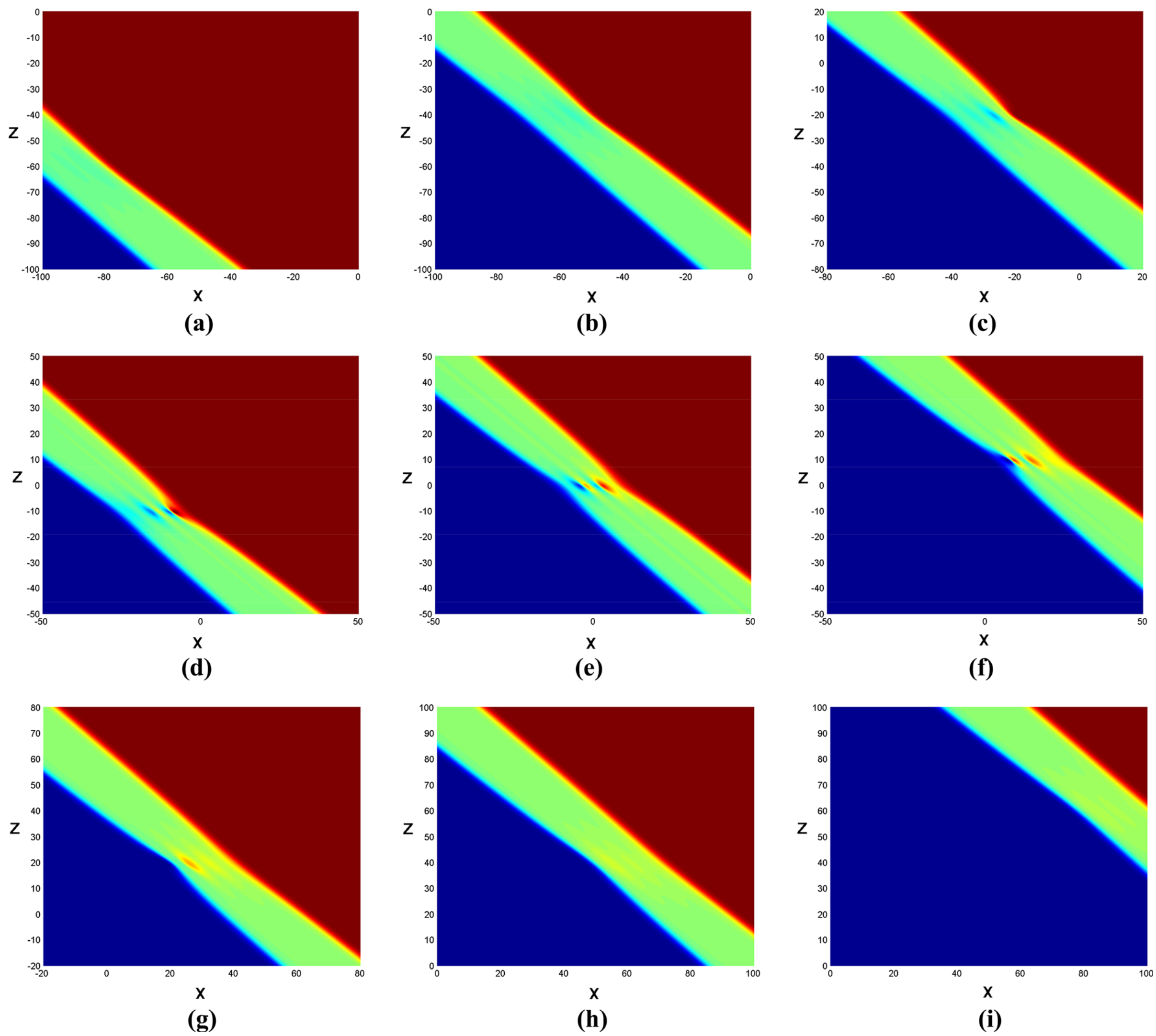

Fig. 4 The contour plot of u via Eq. (32) at **a** $t=-30$, **b** $t=-20$, **c** $t=-10$, **d** $t=-5$, **e** $t=0$, **f** $t=5$, **g** $t=10$, **h** $t=20$ and **i** $t=30$ with $y=0$, $a_1=1$, $a_5=1$, $a_7=3$, $a_8=2$, $a_{10}=1$, $a_{11}=1$, $a_{15}=1$, $a_{16}=1$, $a_{20}=1$, $a_{21}=10$, $k=0.01$ and $l=8$

Based on the differential rules of Pfaffian [38,39], the derivatives of f_N are deduced as

$$
\begin{aligned}
f_{N,x} &= (d_0, d_1, \bullet),\\
f_{N,xx} &= (d_0, d_2, \bullet),\\
f_{N,xxx} &= (d_1, d_2, \bullet) + (d_0, d_3, \bullet),\\
f_{N,y} &= (k^2-1)(d_{-1}, d_0, \bullet),\\
f_{N,xy} &= (k^2-1)(d_{-1}, d_1, \bullet),\\
f_{N,xxy} &= (k^2-1)[(d_0, d_1, \bullet) + (d_{-1}, d_2, \bullet)],\\
f_{N,xxxy} &= (k^2-1)[2(d_0, d_2, \bullet) + (d_{-1}, d_3, \bullet)\\
&\quad + (d_{-1}, d_0, d_1, d_2, \bullet)],\\
f_{N,z} &= k(d_0, d_1, \bullet),\\
f_{N,zz} &= k^2(d_0, d_2, \bullet),\\
f_{N,t} &= k[(d_0, d_3, \bullet) - 2(d_1, d_2, \bullet)],\\
f_{N,yt} &= (k^2-1)[(d_{-1}, d_3, \bullet) - (d_0, d_2, \bullet)\\
&\quad - 2(d_{-1}, d_0, d_1, d_2, \bullet)],
\end{aligned}
\tag{40}
$$

where $f_N = (1, 2, \ldots 2N) = (\bullet)$.

Substituting the results in Eq. (40) into Eq. (4), we can obtain

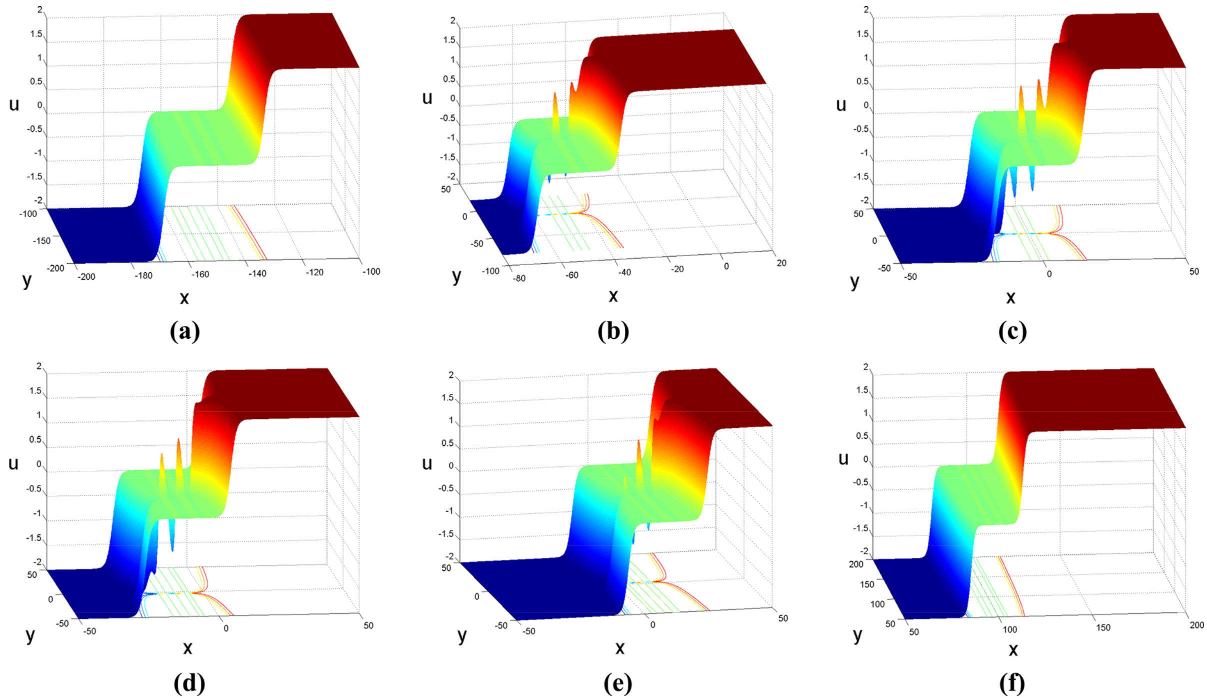

Fig. 5 The 3-dimensional plots of u via Eq. (34) at **a** $t=-30$, **b** $t=-10$, **c** $t=-2$, **d** $t=0$, **e** $t=2$ and **f** $t=20$

$$
\begin{aligned}
&(f_{N,x,x,x,y} - f_{N,y,t} + 3f_{N,x,x} - 3f_{N,z,z})f_N \\
&= 3(k^2-1)(d_{-1}, d_0, d_1, d_2, \bullet)(\bullet), \\
&\quad -3f_{N,x,x,y}f_{N,x} - 3f_{N,x}^2 \\
&= -3(k^2-1)(d_0, d_1, \bullet)(d_{-1}, d_2, \bullet), \\
&f_{N,y}f_{N,t} - f_{N,y}f_{N,x,x,x} = -3(k^2-1)(d_{-1}, d_0, \bullet) \\
&\qquad\qquad (d_1, d(2), \bullet), \\
&3f_{N,x,y}f_{N,x,x} + 3f_{N,z}^2 = 3(k^2-1)(d_0, d_2, \bullet) \\
&\qquad\qquad (d_{-1}, d_1, \bullet),
\end{aligned} \tag{41}
$$

and further, we have

$$
\begin{aligned}
&(D_tD_y - D_x^3D_y - 3D_x^2 + 3D_z^2)f_N \cdot f_N \\
&\quad = \; -6(k^2-1)[(d_{-1}, d_0, d_1, d_2, \bullet)(\bullet) \\
&\qquad - \; (d_{-1}, d_0, \bullet)(d_1, d_2, \bullet) \\
&\qquad + \; (d_{-1}, d_1, \bullet)(d_0, d_2, \bullet) \\
&\qquad - \; (d_{-1}, d_2, \bullet)(d_0, d_1, \bullet)] = 0,
\end{aligned} \tag{42}
$$

which is a Pfaffian identity.

Thus, we can see that f_N is the solution to Eq. (4) and $u = 2(\ln f)_x$ is the solution to Eq. (2). So far, the proof of Theorem 4.1 is finished.

Identically, the bilinear form Eq. (4) can be represented by the following Maya chart.

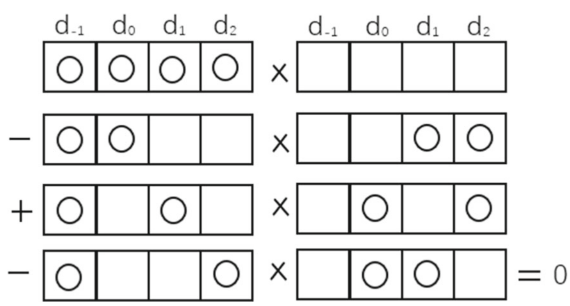

In order to get exact solutions of Eq. (2), we set

$$
\phi_i = e^{\xi_i}, \quad \xi_i = p_i x + (k^2-1)p_i^{-1}y + kp_i z + p_i t + \xi_i^0, \quad i = 1, 2, \cdots, 2N, \tag{43}
$$

where p_i and ξ_i^0 are free parameters.

Now, we set different values to N and various exact solutions to Eq. (2) are obtained.

Setting $N=1$, $c_{12}=1$ and $\phi_j = e^{\xi_j}\,(j=1,2)$, we have

$$
f_1 = (1, 2) = 1 + e^{\eta_1}, \tag{44}
$$

where $\eta_1 = \xi_1 + \xi_2 + \delta_1$, $e^{\delta_1} = \frac{p_1 - p_2}{p_1 + p_2}$.

Based on the expression Eq. (44), the one-soliton solution to Eq. (2) can be written as

$$u = 2(\ln f_1)_x = \frac{2(p_1^2 - p_2^2)e^{\xi_1 + \xi_2}}{(p_1 + p_2) + (p_1 - p_2)e^{\xi_1 + \xi_2}}. \quad (45)$$

Setting $N = 2$ and taking $c_{12} = c_{34} = 1$, $c_{13} = c_{14} = c_{23} = c_{24} = 0$ and $\phi_j = e^{\xi_j} (j = 1, 2, 3, 4)$, we can obtain

$$\begin{aligned} f_2 &= (1, 2, 3, 4) \\ &= (1, 2)(3, 4) - (1, 3)(2, 4) + (1, 4)(2, 3) \\ &= 1 + e^{\eta_1} + e^{\eta_2} + w_{12}e^{\eta_1 + \eta_2}, \end{aligned} \quad (46)$$

where $\eta_1 = \xi_1 + \xi_2 + \delta_1$, $\eta_2 = \xi_3 + \xi_4 + \delta_2$, $e^{\delta_1} = \frac{p_1 - p_2}{p_1 + p_2}$ and $e^{\delta_2} = \frac{p_3 - p_4}{p_3 + p_4}$.

The nonlinear dispersion relation is satisfied automatically, and the phase shift w_{12} is

$$w_{12} = \frac{(p_1 - p_3)(p_1 - p_4)(p_2 - p_3)(p_2 - p_4)}{(p_1 + p_3)(p_1 + p_4)(p_2 + p_3)(p_2 + p_4)}. \quad (47)$$

It is not difficult to find that the form of two-soliton solution is consistent with that obtained by perturbation method [12], where u is expanded as

$$u = \varepsilon u_1 + \varepsilon^2 u_2 + \varepsilon^3 u_3 + \cdots. \quad (48)$$

Further, the two-soliton solution to Eq. (2) is given as

$$u = 2(\ln f_2)_x = \frac{2((p_1 - p_2)e^{\xi_1 + \xi_2} + (p_3 - p_4)e^{\xi_3 + \xi_4} + w_{12}(p_1 + p_2 + p_3 + p_4)e^{\eta_1 + \eta_2})}{1 + e^{\eta_1} + e^{\eta_2} + w_{12}e^{\eta_1 + \eta_2}}. \quad (49)$$

We can obtain the three-soliton solution to Eq. (2) in a similar way. Setting $N = 3$, $c_{12} = c_{34} = c_{56} = 1$, the rest of $c_{ij} = 0$ $(i, j = 1, 2, \cdots, 6)$ and $\phi_j = e^{\xi_j}$ $(j = 1, 2, \cdots, 6)$, f_3 is deduced as

$$\begin{aligned} f_3 &= (1, 2, 3, 4, 5, 6) \\ &= (1, 2)(3, 4, 5, 6) - (1, 3)(2, 4, 5, 6) \\ &\quad + (1, 4)(2, 3, 5, 6) - (1, 5)(2, 3, 4, 6) \\ &\quad + (1, 6)(2, 3, 4, 5) \\ &= (1, 2)(3, 4)(5, 6) - (1, 2)(3, 5)(4, 6) \\ &\quad + (1, 2)(3, 6)(4, 5) - (1, 3)(2, 4)(5, 6) \\ &\quad + (1, 3)(2, 5)(4, 6) - (1, 3)(2, 6)(4, 5) \\ &\quad + (1, 4)(2, 3)(5, 6) - (1, 4)(2, 5)(3, 6) \\ &\quad + (1, 4)(2, 6)(3, 5) - (1, 5)(2, 3)(4, 6) \\ &\quad + (1, 5)(2, 4)(3, 6) - (1, 5)(2, 6)(3, 4) \\ &\quad + (1, 6)(2, 3)(4, 5) - (1, 6)(2, 4)(3, 5) \\ &\quad + (1, 6)(2, 5)(3, 4). \end{aligned} \quad (50)$$

Likewise, we may rewrite f_3 as

$$\begin{aligned} f_3 &= 1 + e^{\eta_1} + e^{\eta_2} + e^{\eta_3} + w_{12}e^{\eta_1 + \eta_2} + w_{13}e^{\eta_1 + \eta_3} \\ &\quad + w_{23}e^{\eta_2 + \eta_3} + w_{12}w_{13}w_{23}e^{\eta_1 + \eta_2 + \eta_3}, \end{aligned} \quad (51)$$

where

$$\begin{aligned} &\eta_3 = \xi_5 + \xi_6 + \delta_3, \; e^{\delta_3} = \frac{p_5 - p_6}{p_5 + p_6}, \\ &w_{13} = \frac{(p_1 - p_5)(p_1 - p_6)(p_2 - p_5)(p_2 - p_6)}{(p_1 + p_5)(p_1 + p_6)(p_2 + p_5)(p_2 + p_6)}, \\ &w_{23} = \frac{(p_3 - p_5)(p_3 - p_6)(p_4 - p_5)(p_4 - p_6)}{(p_3 + p_5)(p_3 + p_6)(p_4 + p_5)(p_4 + p_6)}, \end{aligned} \quad (52)$$

and the three-soliton solution to Eq. (2) can be derived as $u = 2(\ln f_3)_x$. Selecting appropriate parameters, the one-, two- and three-soliton solutions are given in Fig. 6. The contour plots of one-, two- and three-soliton solutions are plotted in Fig. 7.

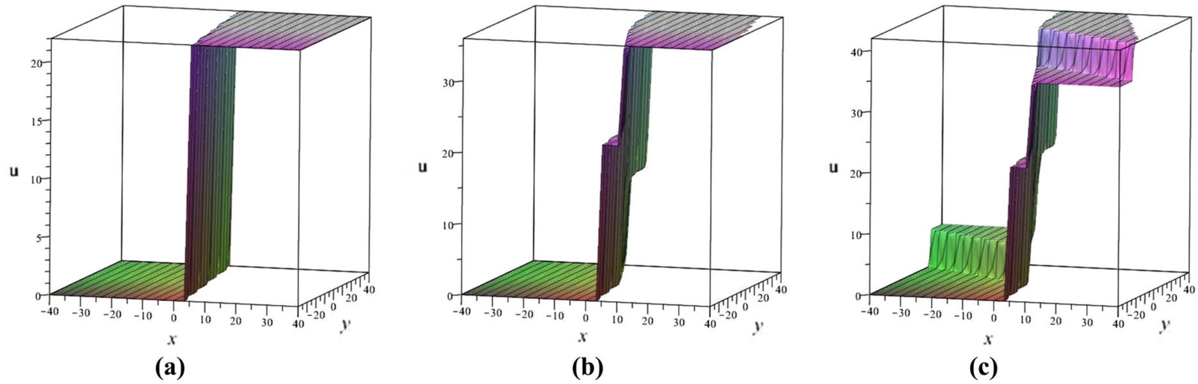

Fig. 6 One-, two- and three-soliton solutions to Eq. (2) at $t = 0$ with $z = 0$, $p_1 = 6$, $p_2 = 5$, $p_3 = 4$, $p_4 = 3$, $p_5 = 2$, $p_6 = 1$, $\xi_1^0 = 0$, $\xi_2^0 = 0$, $\xi_3^0 = 0$, $\xi_4^0 = 0$, $\xi_5^0 = 0$, $\xi_6^0 = 0$ and $k = 2$

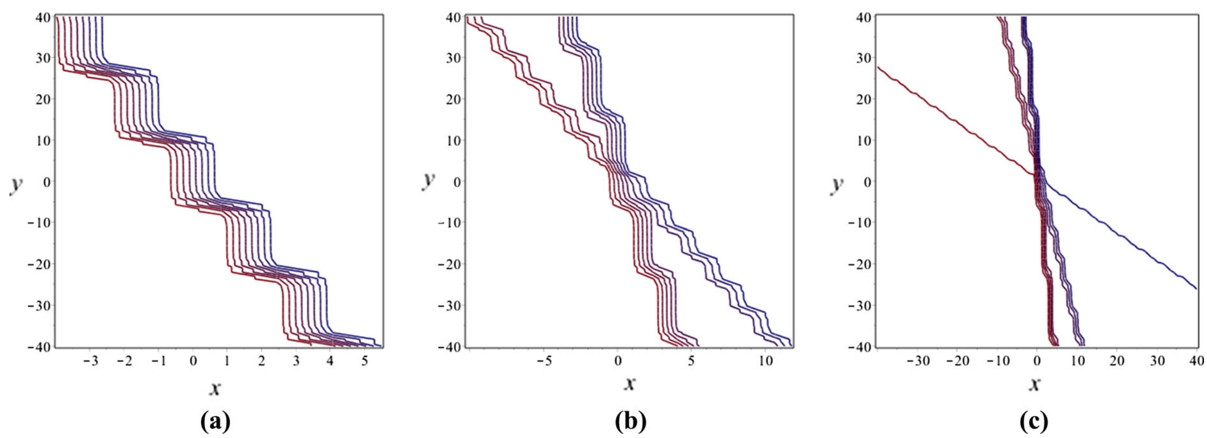

Fig. 7 Contour plots of one-, two- and three-soliton solutions to Eq. (2) at $t = 0$ with $z = 0$, $p_1 = 6$, $p_2 = 5$, $p_3 = 4$, $p_4 = 3$, $p_5 = 2$, $p_6 = 1$, $\xi_1^0 = 0$, $\xi_2^0 = 0$, $\xi_3^0 = 0$, $\xi_4^0 = 0$, $\xi_5^0 = 0$, $\xi_6^0 = 0$ and $k = 2$

5 Conclusions

In this paper, a (3+1)-dimensional nonlinear partial differential equation has been transformed into Hirota bilinear form by applying a transformation [see Eq. (3)]. A bilinear BT Eq. (9) which consists of four bilinear equations and involves six arbitrary parameters was then constructed. Based on the constructed BT, one-soliton solution to Eq. (2) was derived. Using the test function method, we have obtained three sets of lump–kink solutions and have investigated new-type interaction solutions via the test function expressed by "polynomial-cos-cosh." Analyzing the complex interaction phenomena of waves is evocative and delightful. Based on the solutions Eqs. (19), (32) and (34), abundant interaction phenomena related to lump wave, trigonometric-type wave and kinky wave have been displayed and the periodic phenomenon has also been revealed. In the meantime, we have obtained the interaction wave combined by x-periodic lump wave and two-kinky wave. Moreover, Pfaffian solutions to Eq. (2) have been constructed based on Theorem (4.1). Setting different values to N and selecting appropriate parameters, one-, two- and three-soliton solutions are derived. In general, various exact solutions to a (3+1)-dimensional NLEE have been obtained and discussed in this paper, which provides useful methods for reference. It is worth noticing that more exact solutions which possess crucial properties can be deduced through symbolic computation in future study and the application of the Bäcklund transformation provides approaches to deriving new solutions based on known ones. The result of our research helps explain nonlinear phenomena and can be applied in fluid mechanics.

Acknowledgements This work is supported by the Project of National Training Program of Innovation and Entrepreneurship for Postgraduates (2021YJS172) and the National Natural Science Foundation of China under Grant No. 71971015.

Declarations

Conflicts of interest The authors declare that they have no conflict of interest.

Data availability statement Our manuscript has no associated data.

References

1. Lonngren, K.E.: Ion acoustic soliton experiments in a plasma. Opt. Quantum Electron **30**, 615 (1998)
2. Seadawy, A.R.: Stability analysis for Zakharov-Kuznetsov equation of weakly nonlinear ion-acoustic waves in a plasma. Comput. Math. Appl. **67**, 172 (2014)
3. Dai, C.Q., Wang, Y.Y.: Coupled spatial periodic waves and solitons in the photovoltaic photorefractive crystals. Nonlinear Dyn. 102, 1733 (2020)
4. Lü, X., Ma, W.X., Yu, J., Khalique, C.M.: Solitary waves with the Madelung fluid description: a generalized derivative nonlinear Schr*ö*dinger equation. Commun. Nonlinear Sci. Numer. Simul. **31**, 40 (2016)
5. Liu, L., Zhu, L.L., Yang, D.: Modeling and simulation of the car-truck heterogeneous traffic flow based on a nonlinear car-following model. Appl. Math. Comput. **273**, 706 (2016)
6. Nagatani, T.: Traffic flow on star graph: nonlinear diffusion. Physica A **561**, 125251 (2021)
7. Guo, H., Xiao, X.P.: Urban road short-term traffic flow forecasting based on the delay and nonlinear grey model. J. Transp. Syst. Eng. Inf. Technol. **13**, 60 (2013)
8. Bhrawy, A.H., Abdelkawy, M.A., Biswas, A.: Topological solitons and cnoidal waves to a few nonlinear wave equations in theoretical physics. Indian J. Phys. **87**, 1125 (2013)
9. Li, H., Xu, S.L.: Three-dimensional solitons in Bose-Einstein condensates with spin-orbit coupling and Bessel optical lattices. Phys. Rev. A **98**, 033827 (2018)
10. Guo, Y.W., Xu, S.L.: Transient optical response of cold Rydberg atoms with electromagnetically induced transparency. Phys. Rev. A **101**, 023806 (2020)
11. Xu, S.L., Li, H., Zhou, Q.: Parity-time symmetry light bullets in a cold Rydberg atomic gas. Opt. Express **28**, 16322–16332 (2020)
12. Hirota, R.: The Direct Method in Soliton Theory. Cambridge Univ. Press, Cambridge (2004)
13. Xia, J.W., Zhao, Y.W., Lü, X.: Predictability, fast calculation and simulation for the interaction solutions to the cylindrical Kadomtsev-Petviashvili equation. Commun. Nonlinear Sci. Numer. Simul. **90**, 105260 (2020)
14. Chen, S.J., Lü, X.: Novel evolutionary behaviors of the mixed solutions to a generalized Burgers equation with variable coefficients. Commun. Nonlinear Sci. Numer. Simul. **95**, 105628 (2021)
15. He, X. J., Lü, X.: B*ä*cklund transformation, Pfaffian, Wronskian and Grammian solutions to the (3+1)-dimensional generalized Kadomtsev-Petviashvili equation. Analysis and Mathematical Physics, **11**, No.4 (2020)
16. Meng, Q.: Rational solutions and interaction solutions for a fourth-order nonlinear generalized Boussinesq water wave equation. Appl. Math. Lett. **110**, 106580 (2020)
17. Hua, Y.F.: Interaction behavior associated with a generalized (2+1)-dimensional Hirota bilinear equation for nonlinear waves. Appl. Math. Model. **74**, 185 (2019)
18. Liu, N., Liu, Y.S.: New multi-soliton solutions of a (3+1)-dimensional nonlinear evolution equation. Comput. Math. Appl. **71**, 1645 (2016)
19. Lü, X., Ma, W.X.: Study of lump dynamics based on a dimensionally reduced Hirota bilinear equation. Nonlinear Dyn. **85**, 1217 (2016)
20. Dai, C.Q., Wang, Y.Y., Zhang, X.F.: Spatiotemporal localizations in (3+1)-dimensional PT-symmetric and strongly nonlocal nonlinear media. Nonlinear Dyn. **83**, 2453 (2016)
21. Lü, X., Ma, W.X., Yu, J., Lin, F.H., Khalique, C.M.: Envelope bright- and dark-soliton solutions for the Gerdjikov-Ivanov model. Nonlinear Dyn. **82**, 1211 (2015)
22. Yin, Y.H., Chen, S.J., Lü, X.: Study on localized characteristics of lump and interaction solutions to two extended Jimbo-Miwa equations. Chin. Phys. B **29**, 120502 (2020)
23. Lü, X., Chen, S.J.: Interaction solutions to nonlinear partial differential equations via Hirota bilinear forms: One-lump-multi-stripe and one-lump-multi-soliton types. Nonlinear Dyn. **103**, 947 (2021)
24. Ma, W.X., Fan, E.G.: Linear superposition principle applying to Hirota bilinear equations. Comp. Math. Appl. **61**, 950 (2011)
25. Ma, W.X., Zhang, Y., Tang, Y.N., Tu, J.Y.: Hirota bilinear equations with linear subspaces of solutions. Appl. Math. Comput. **218**, 7174 (2012)
26. Ma, W.X., Abdeljabbar, A.: A bilinear Backlund transformation of a (3+1)-dimensional generalized KP equation. Appl. Math. Lett. **25**, 1500 (2012)
27. Ma, W.X., Qin, Z.Y., Lü, X.: Lump solutions to dimensionally reduced p-gKP and p-gBKP equations. Nonlinear Dyn. **84**, 923 (2016)
28. Ma, W.X.: Lump solutions to the Kadomtsev-Petviashvili equation. Phys. Lett. A **379**, 1975 (2015)
29. Chen, S.J., Lü, X, Li, M. G., Wang, F.: Derivation and simulation of the M-lump solutions to two(2+1)-dimensional nonlinear equations. Phys. Scr. **96**, 095201 (2021)
30. Li, L.F., Xie, Y.Y., Mei, L.Q.: Multiple-order rogue waves for the generalized (2+1)-dimensional Kadomtsev-Petviashvili equation. Appl. Math. Lett. **117**, 107079 (2021)
31. Lü, X., Hua, Y.F., Chen, S.J., Tang, X.F.: Integrability characteristics of a novel (2+1)-dimensional nonlinear model: Painlevé analysis, soliton solutions, Bäcklund transformation, Lax pair and infinitely many conservation laws. Commun. Nonlinear Sci. Numer. Simul. **95**, 105612 (2021)
32. Zha, Q.L.: Rogue waves and rational solutions of a (3+1)-dimensional nonlinear evolution equation. Phys. Lett. A **377**, 3021 (2013)

33. Geng, X.G., Ma, Y.L.: N-soliton solution and its Wronskian form of a (3+1)-dimensional nonlinear evolution equation. Phys. Lett. A **369**, 285 (2007)
34. Xu, H.N., Ruan, W.Y., Zhang, Y., Lü, X.: Multi-exponential wave solutions to two extended Jimbo-Miwa equations and the resonance behavior. Appl. Math. Lett. **99**, 105976 (2020)
35. Nimmo, J.J.C., Freeman, N.C.: A method of obtaining the N-soliton solution of the Boussinesq equation in terms of a wronskian. Phys. Lett. A **95**, 4 (1983)
36. Li, C.X., Zeng, Y.B.: Soliton solutions to a higher order Ito equation: Pfaffian technique. Phys. Lett. A **363**, 4 (2007)
37. Ohta, Y.: Pfaffian solution for coupled discrete nonlinear Schr*ö*dinger equation. Chaos, Solitons Fractals **11**, 91 (2000)
38. Tang, Y.N.: Pfaffian solutions and extended Pfaffian solutions to (3+1)-dimensional Jimbo-Miwa equation. Appl. Math. Mode **37**, 6632 (2013)
39. Ohta, Y.: Pfaffian solution for coupled discrete nonlinear Schr*ö*dinger equation. Chaos, Solitons Fractals **11**, 92 (2000)
40. Hirota, R.: Soliton solutions to the BKP equations-I. The Pfaffian technique, J. Phys. Soc. Jpn., **58**, 2286 (1989)
41. Chen, S.J., Ma, W.X., Lü, X.: Bäcklund transformation, exact solutions and interaction behaviour of the (3+1)-dimensional Hirota-Satsuma-Ito-like equation. Commun. Nonlinear Sci. Numer. Simul. **83**, 105135 (2020)
42. Gao, L.N., Zhao, X.Y., Zi, Y.Y., Yu, J., Lü, X.: Resonant behavior of multiple wave solutions to a Hirota bilinear equation. Comp. Math. Appl. **72**, 1225 (2016)
43. Fang, T., Wang, Y.H.: Interaction solutions for a dimensionally reduced Hirota bilinear equation. Comput. Math. Appl. **76**, 1476 (2018)
44. Saha, A.: Dynamics of the generalized KP-MEW-Burgers equation with external periodic perturbation. Computers Mathematics with Applications **73**, 1880 (2017)
45. Abdel-Gawad, H.I., Tantawy, M.: Two-layer fluid formation and propagation of periodic solitons induced by (3+1)-dimensional KP equation. Computers Mathematics with Applications **78**, 2011 (2019)
46. Zhang, H.Y., Zhang, Y.F.: Analysis on the M-rogue wave solutions of a generalized (3+1)-dimensional KP equation. Appl. Math. Lett. **102**, 106145 (2020)